

# Hard X-ray richness of weak flares – Joint STIX, SDO analysis

**Arun Kumar Awasthi**  
**arun@cbk.pan.wroc.pl**

*Space Research Centre Solar Physics Division, Polish Academy of Sciences  
ul. Kopernika 11, 51-622 Wrocław, Poland*

STIX Meeting – Wrocław

Date: November 8, 2023



This project has received funding from the European Union's Horizon 2020 research and innovation programme under the Maria Skłodowska-Curie grant agreement No 847639.

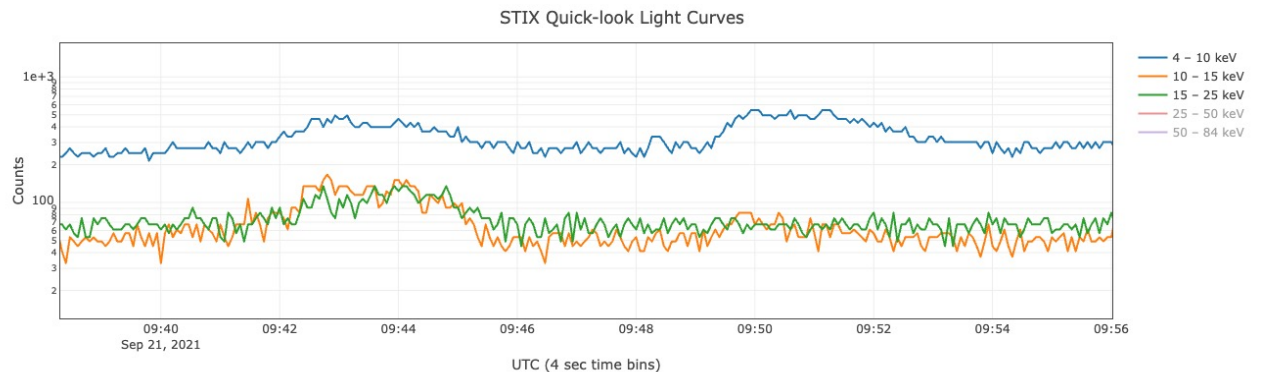
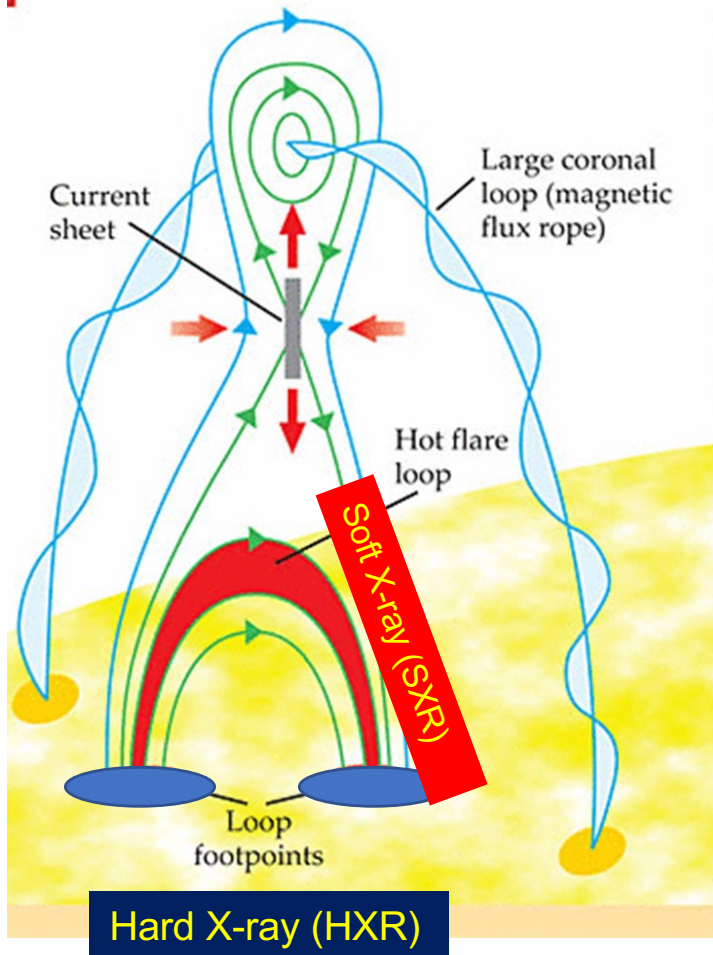
Maria Skłodowska-Curie Actions

# Thermal-Nonthermal Emission during flares

**(Empirical) Neupert effect (ENE)** – Time derivative of soft X-ray flux  $F_{SXR}(t)$  mimics hard X-ray flux  $F_{HXR}(t)$  in time.

$$F_{SXR}(t_p) \propto \int_{t_0}^{t_p} F_{HXR}(t) dt$$

**Theoretical Neupert effect (TNE)** - Beam power supply  $P_{beam}(t)$  (from the hard X-ray spectrum) should match the actual power  $P_{in}(t)$  required to explain the soft X-ray flux and spectrum (Veronig et al. 2005). TNE did not reveal a better correlation than ENE.



# Context

---

McTiernan et al. (1999)

- Through differential emission measure (DEM) of YOHKOH/SXT and BCS observed flares, flares with **high-temperature plasma** ( $\geq 16.5\text{MK}$ ) exhibited the Neupert effect.

Lysenko et al. (2020)

- Early impulsive (cold) flares, originate from shorter loops with a stronger magnetic field compared to the average geometrical properties of analyzed flares.

Motorina et al. (2020) & Fleishman et al. (2021)

- **Magnetic structure + initial distribution of the thermal plasma parameters** - decide how the released energy is apportioned between the thermal and nonthermal components.

Fleishman et al. (2022)

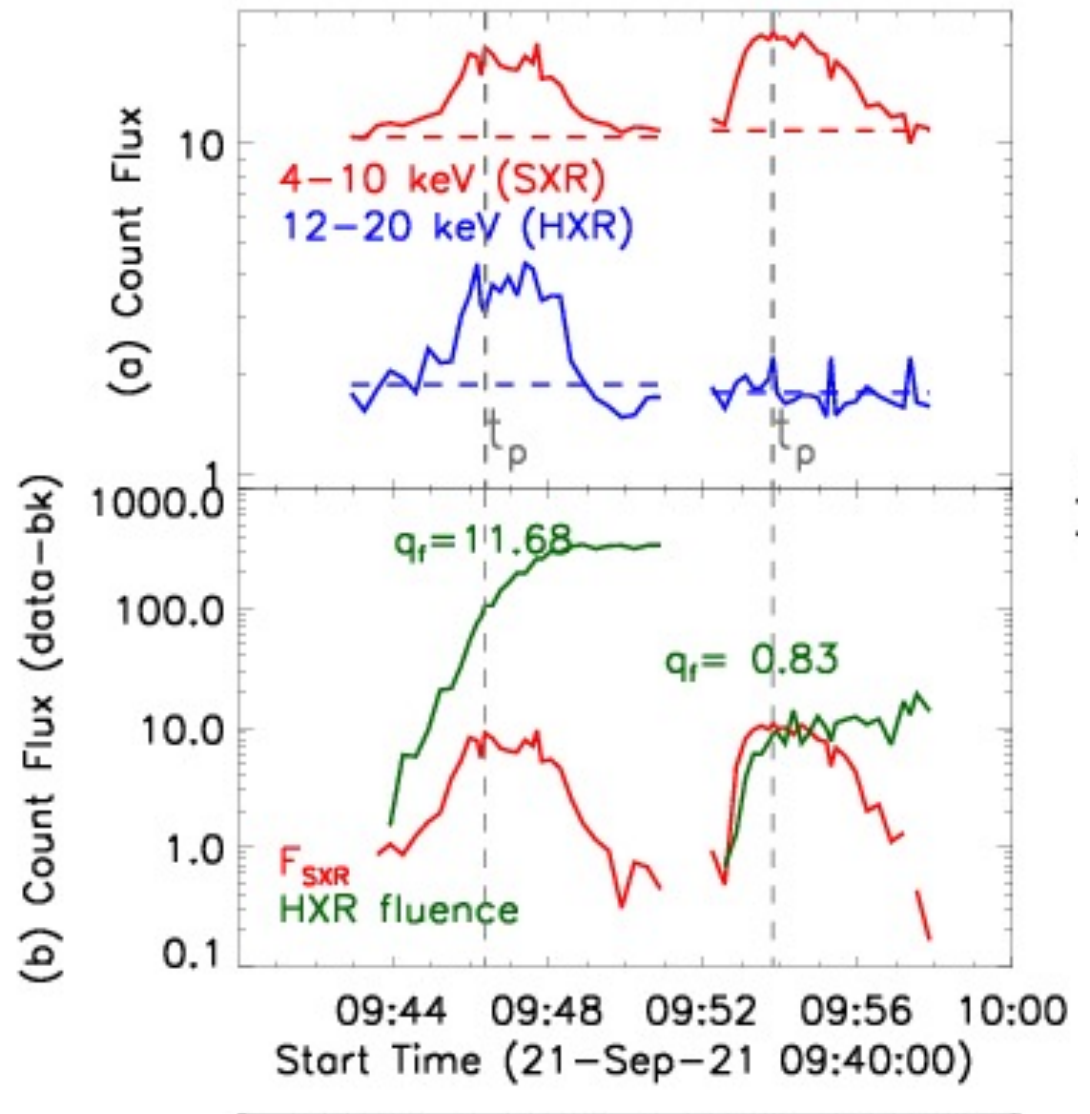
- **Hard X-rays**, produced by high-energy electrons accelerated in the flare, **require a high ambient density** for their detection.

# HXR-richness / Relative Yield of HXR emission

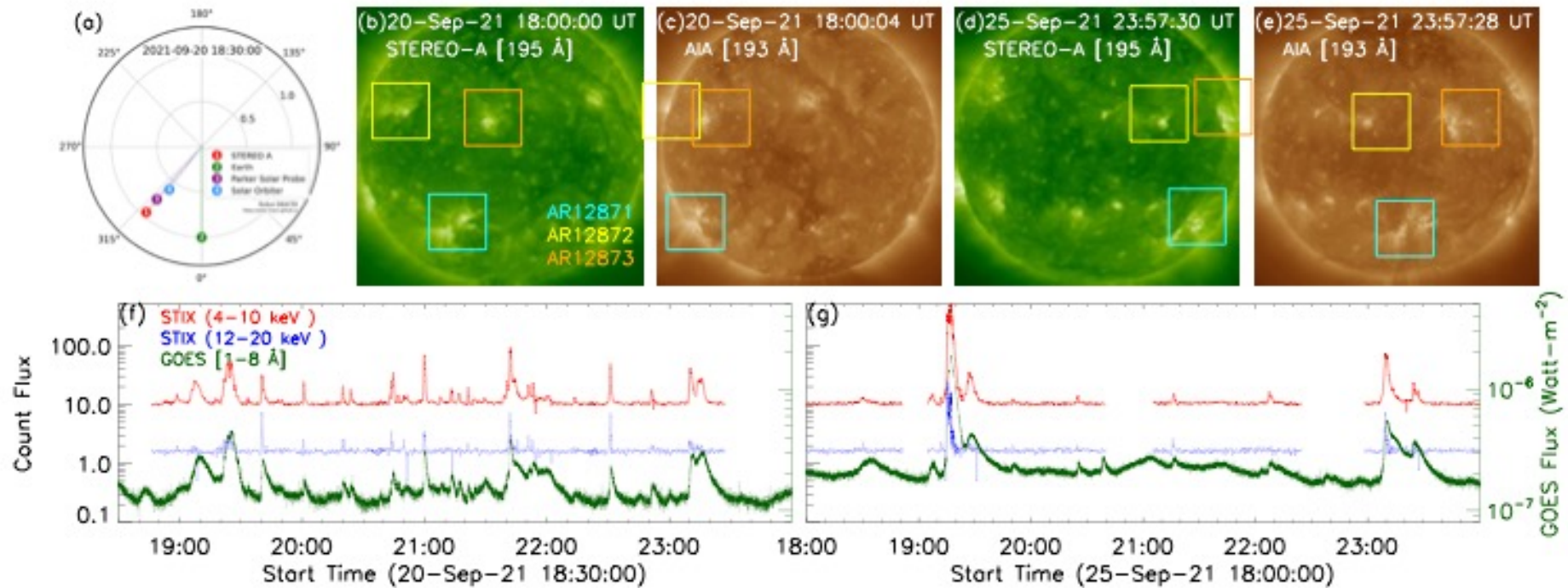
Quantifying the relative (nonthermal) productivity of flare –

$$q_f(t_p) = \frac{\int_{t_0}^{t_p} F_{HXR}(t) dt}{F_{SXR}(t_p)}$$

Here,  $t_0$  and  $t_p$  correspond to the start and peak time of  $F_{SXR}$ , respectively.

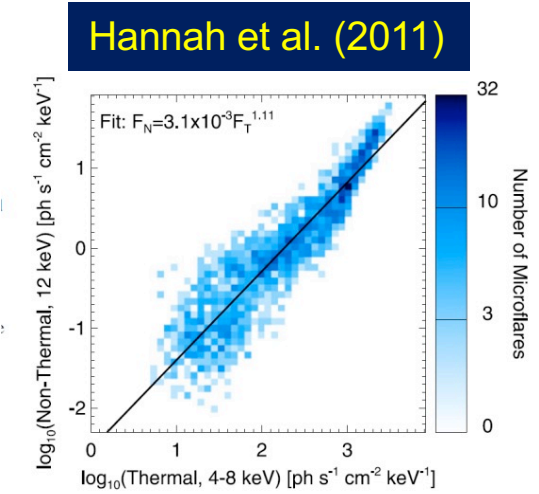
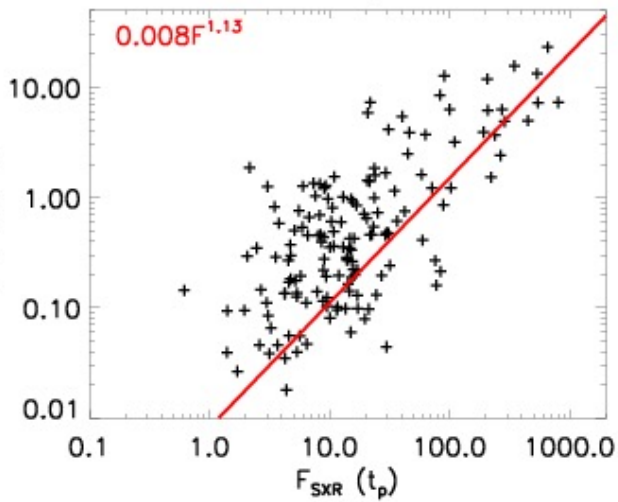
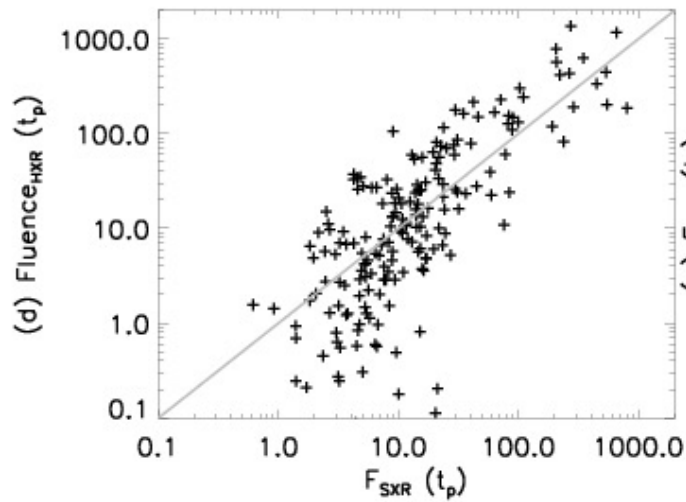


# Observations

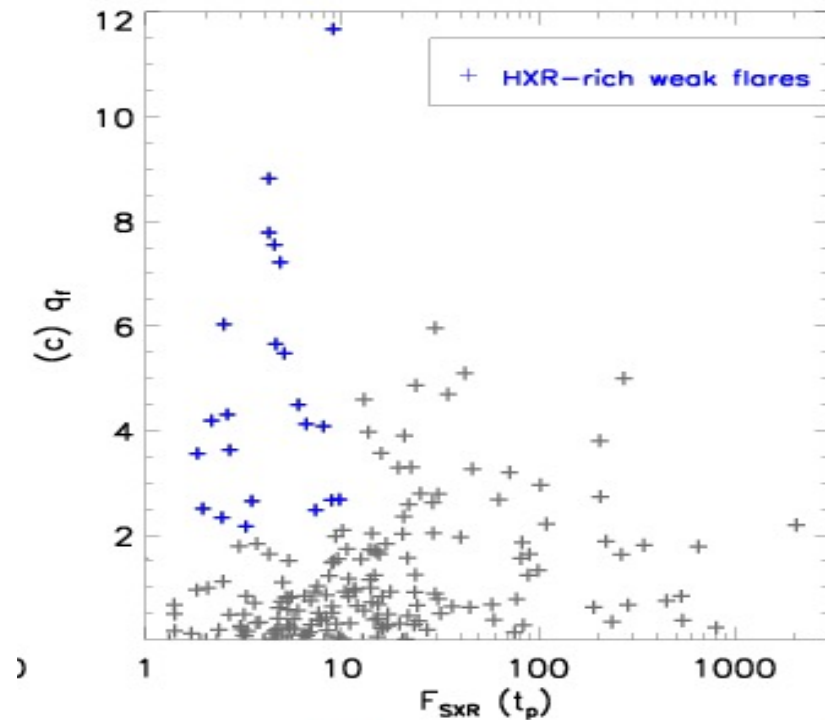


From STEREO-A and SDO, and X-ray intensity evolution in 4-10 keV, and 12-20 keV, from the quick-look mode observations from STIX instrument, and in 1–8 Å from GOES mission, overlapping observations of flare events recorded by instruments positioned at different vantage points.

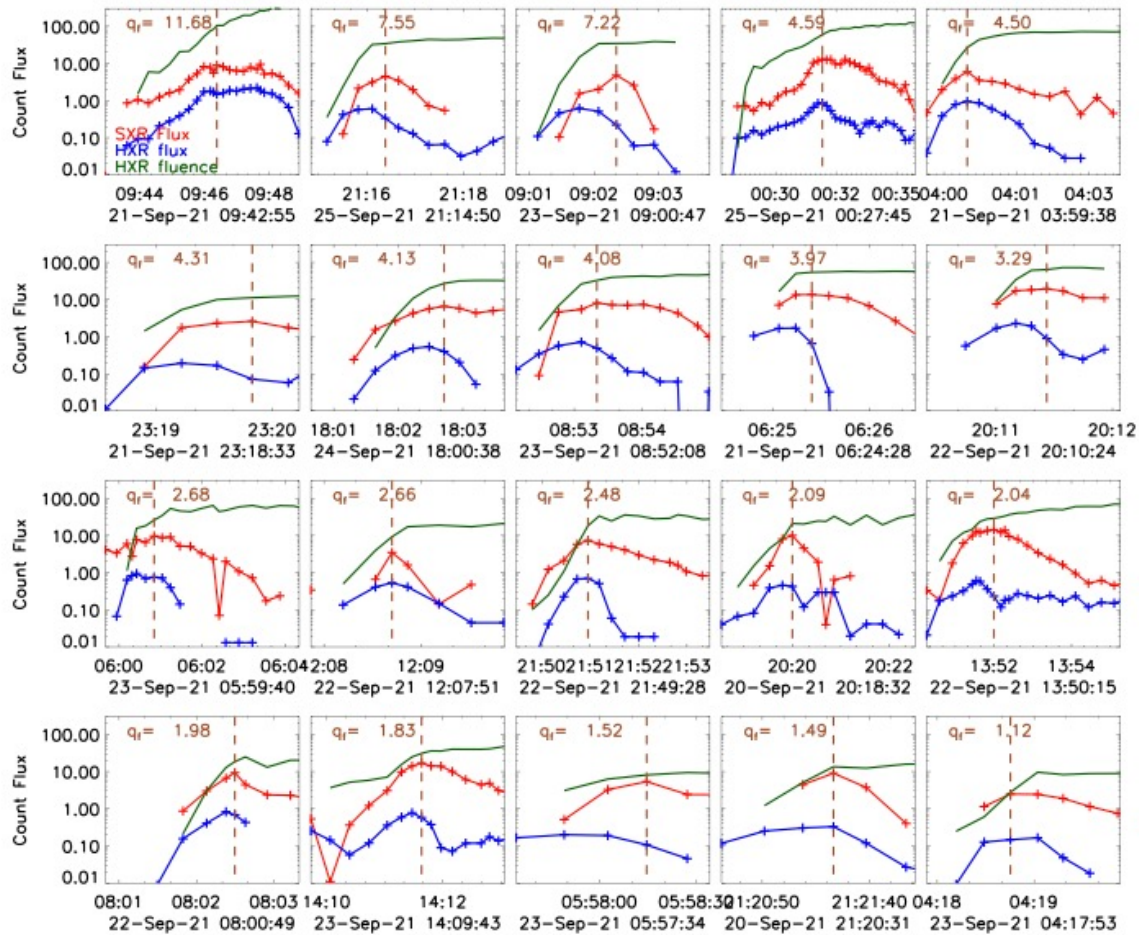
# A statistical look at the temporal characteristics



Variation of the relative yield of HXR emission ( $q_f$ ) with respect to the peak SXR flux enabled us to select 20 HXR-rich weak flare cases



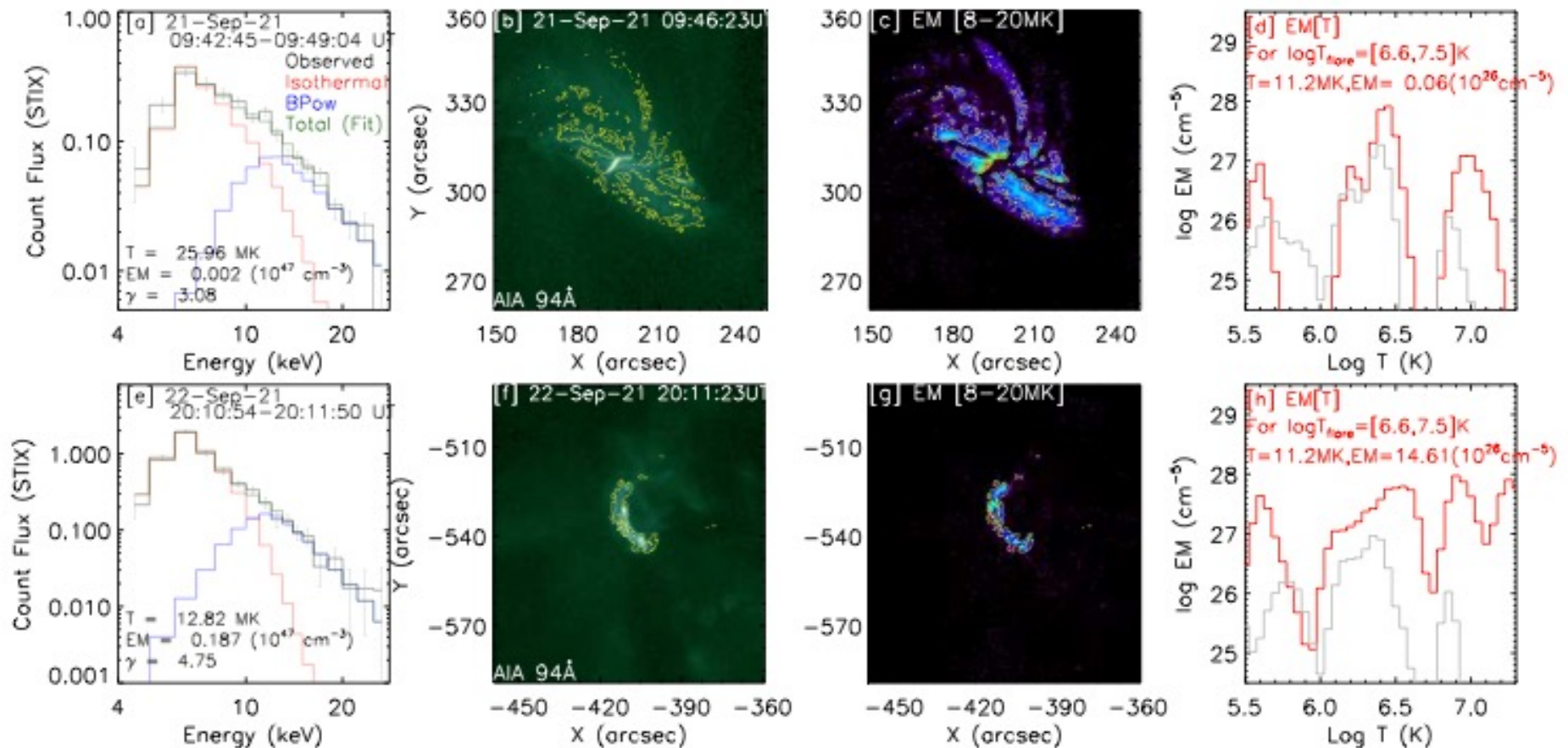
# Flare cases with strong nonthermal emission



Very similar 4-10 keV Peak flux

S.N.	Flare	$F_{SXR}^a$	$q_f$
1	SOL2021-09-21T09:46:22	19.5(10.5)	11.68
2	SOL2021-09-25T21:16:23	15.3(10.8)	7.55
3	SOL2021-09-23T09:02:20	15.9(11.1)	7.22
4	SOL2021-09-25T00:31:55	23.3(10.4)	4.59
5	SOL2021-09-21T04:00:28	16.9(10.9)	4.50
6	SOL2021-09-21T23:19:49	13.4(10.8)	4.31
7	SOL2021-09-24T18:02:42	17.4(10.8)	4.13
8	SOL2021-09-23T08:53:19	18.7(10.7)	4.08
9	SOL2021-09-21T06:25:24	24.4(10.9)	3.97
10	SOL2021-09-22T20:11:26	30.9(11.5)	3.29
11	SOL2021-09-23T06:00:50	21.3(11.6)	2.68
12	SOL2021-09-22T12:08:42	14.0(10.5)	2.66
13	SOL2021-09-22T21:50:57	17.8(10.4)	2.48
14	SOL2021-09-20T20:19:59	20.7(10.6)	2.09
15	SOL2021-09-22T13:51:59	24.7(10.5)	2.04
16	SOL2021-09-22T08:02:29	20.4(11.1)	1.98
17	SOL2021-09-23T14:11:38	26.9(10.2)	1.83
18	SOL2021-09-23T05:58:14	21.5(16.2)	1.52
19	SOL2021-09-20T21:21:23	19.4(10.4)	1.49
20	SOL2021-09-23T04:18:45	16.1(13.6)	1.12

# Thermal characteristics from X-ray and EUV

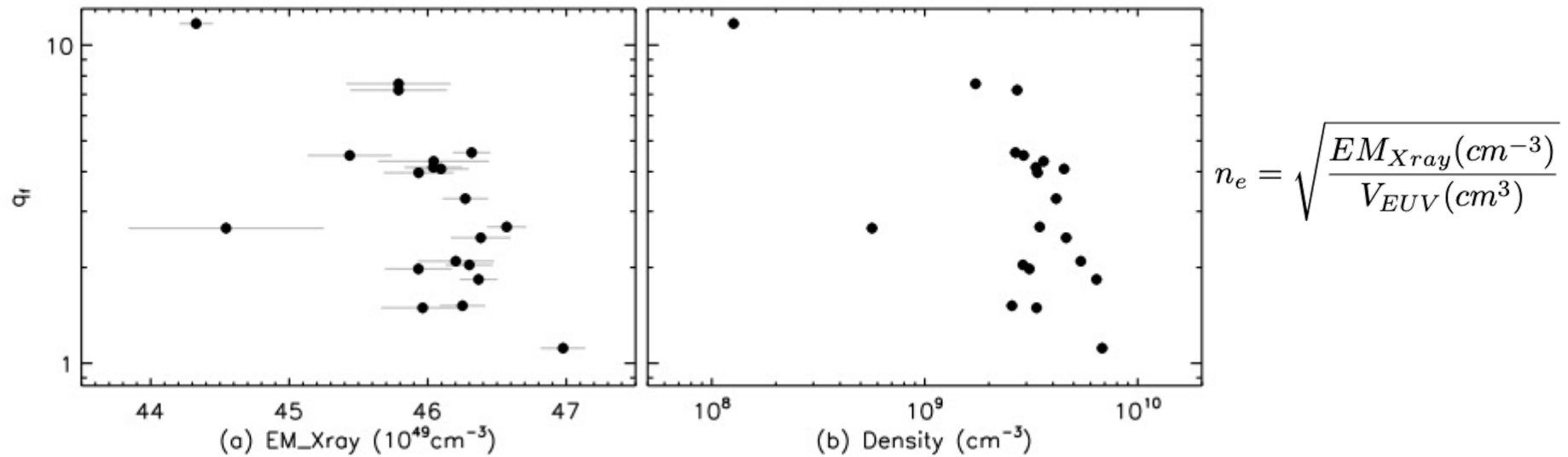


- From the 8–20 MK EM map, the flare region  $\Rightarrow EM > 10^{26} \text{ cm}^{-5}$

- $\log T = [6.6, 7.5]$  
$$T_{EM} = \frac{\sum_j T_j \times EM(T_j)}{\sum_j EM(T_j)}$$

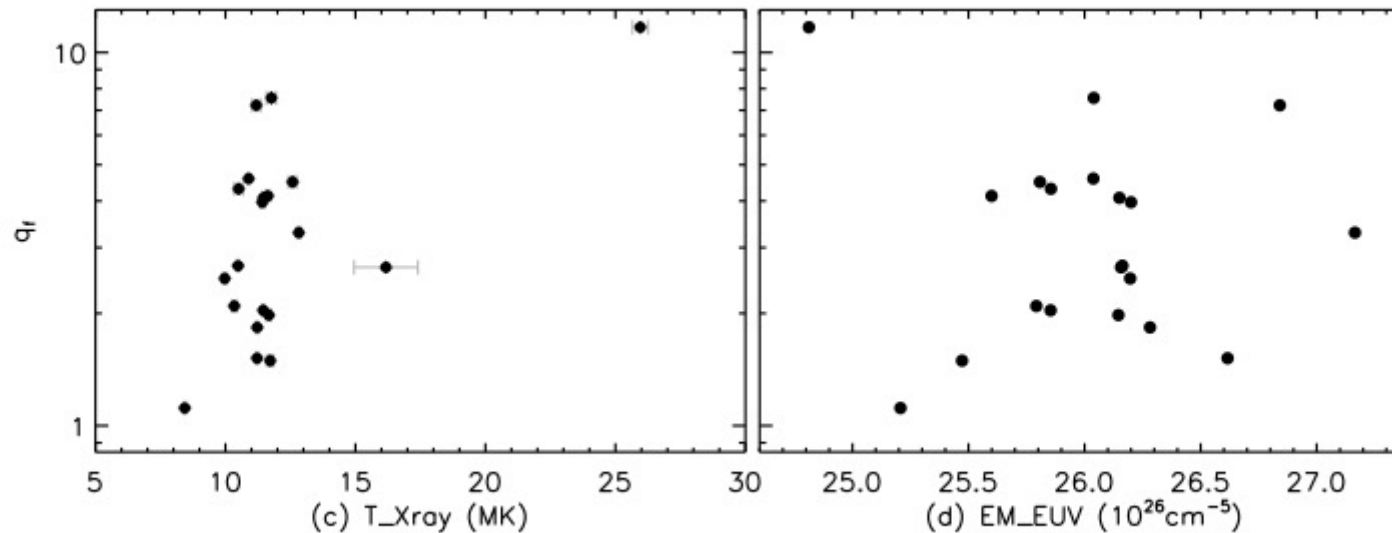


# HXR-richness and flare parameters



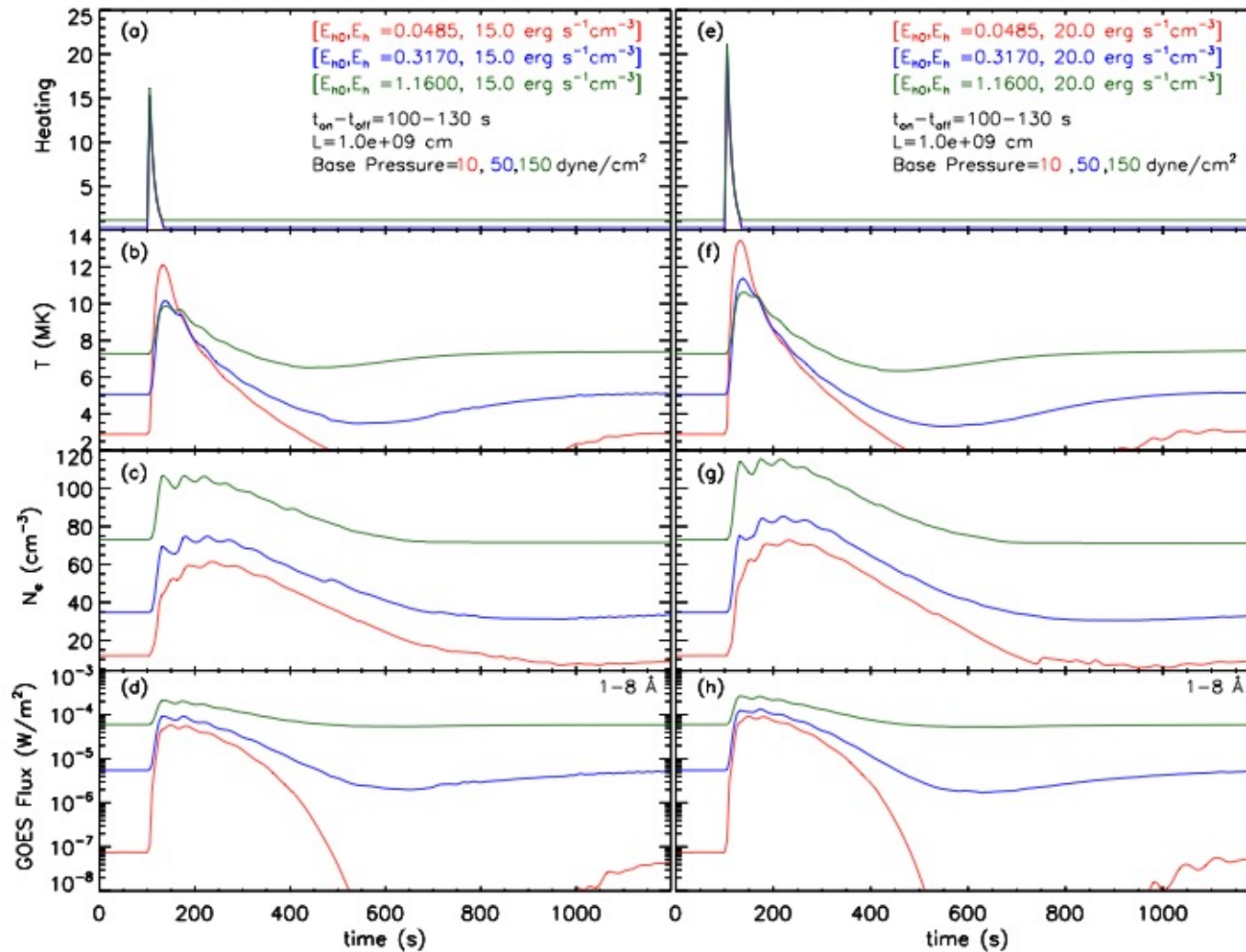
- We find the derived EM and  $n_e$  to be **inversely related to  $q_f$** , i.e., the emission measure of the flare plasma is lower in the case of flares exhibiting relatively larger HXR yield and vice-versa.

# HXR-richness and flare parameters



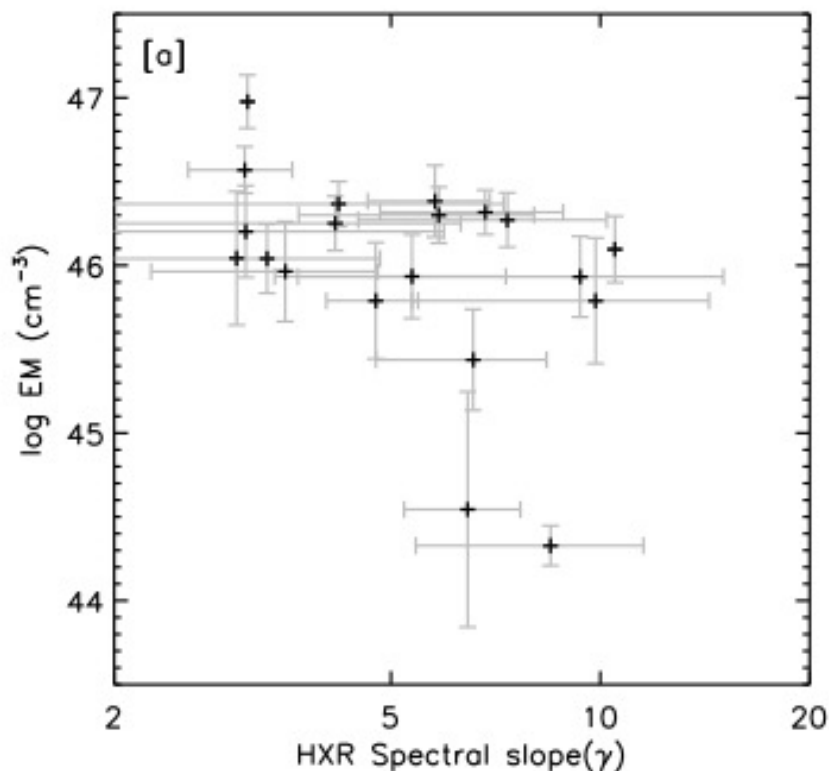
- Plasma temperature is found to be **positively correlated** with the HXR-richness of the flares.
- These correlations indicate that the **stronger nonthermal mission heats the flare plasma more efficiently without significantly increasing the plasma density.**
- EUV EM (and temperature) do not exhibit any clear correlation with  $q_f$ .

# Insights from the Palermo-Harvard hydrodynamical code



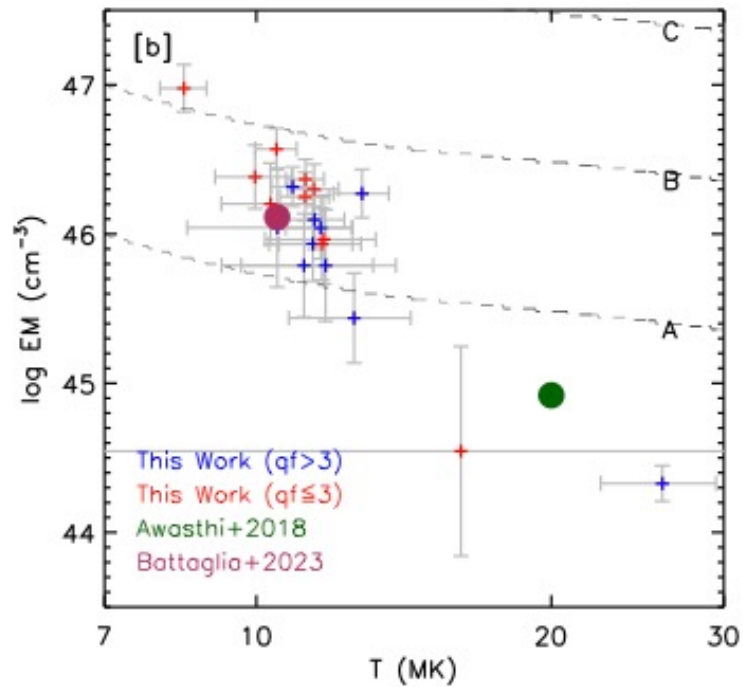
- For the same heating input, loops with **lower base pressure** exhibit plasma of **higher temperature and lower density**.
- In agreement with the implications made from the X-ray spectral analysis of HXR-rich flare cases.

# HXR spectral slope and EM-T map



- Nonthermal electrons with a harder spectrum result in higher EM => explosive chromospheric evaporation (also in Motorina et al's case study).
- Unlike large flares having an inverse relation (lower energy electrons drive up-flows sooner than higher energy electrons).
- Simulation from Reep et al. (2015) indicated that, for weak flares, explosive evaporation threshold can be achieved with very little total nonthermal energy and the thermal response of the atmosphere may not strongly depend on the electron energy in this regime.

# T-EM map and GOES class



- Despite the fact that our work considers flares with **similar peak SXR emission** ( $< 20$  counts  $\text{s}^{-1}\text{cm}^{-2}\text{keV}^{-1}$ ), from the ISO-flux lines for GOES A, B, and C classes, the intensity classes of the analyzed flares **vary between sub-A to B-class**.

